small NANO MICRO

Catalysis

'Click' Preparation of CuPt Nanorod-Anchored Graphene Oxide as a Catalyst in Water

*Hyunseung Yang, Yongwoo Kwon, Taegyun Kwon, Hyunjoo Lee, and Bumjoon J. Kim**

In this paper, a simple and powerful method of producing nanoparticle-anchored graphene oxide (GO) composites using a 'click' reaction is demonstrated. This method affords a facile means of anchoring of nanoparticles with various shapes and sizes on the GO. CuPt nanorods with controlled size, aspect ratio (from 1 to 11), and uniformity are synthesized. Transmission electron microscopy, Fourier transform infrared spectroscopy, and X-ray photoelectron spectroscopy measurements are made to monitor the formation and characterize the properties of the CuPt nanorod-grafted GO composites. Their catalytic properties in the water phase are investigated using an o-phenylenediamine oxidation reaction. The results of this study clearly demonstrate that nonpolar CuPt nanorods immobilized on GO can function as a catalyst in an aqueous solution and that GO can be used as a catalytic nanorod support.

1. Introduction

Metal nanoparticles with well defined shapes and sizes have received considerable attention because of their electrical,[1,2] magnetic,[3,4] and catalytic properties.[5,6] Because the properties of nanoparticles are highly dependent on their size and shape, it is important to precisely control these properties during synthesis.[7] Nanoparticles with a controlled size or shape are typically synthesized by reducing metal precursors in the presence of organic surface-capping agents. The surface-capping agents not only prevent aggregation by stabilizing the nanoparticles but also induce a specific size or shape while interfering in the overgrowth of metal nanoparticles. These surface-capping agents, however, often hinder further applications of the nanoparticles, prohibiting dispersion in other kinds of solvents or making surface functionalization more difficult.[8] Techniques that facilitate simple and universal surface modification are important to various applications.[9–15] In particular, the immobilization of shape-controlled nanoparticles on a support can further extend the potential applications.

Graphene consists of a single layer of sp^2-bonded carbon atoms forming a 2D hexagonal lattice.[16] Because it has a high surface area, flexibility, transparency and excellent electrical and thermal conductivity,[17] graphene is a promising candidate for use as a building block of new functional composite materials.[18] Among the various types of graphene and their derivatives, graphene oxide (GO) is a common choice because of its facile synthetic nature in a controlled scalable and reproducible manner.[19–21] The presence of oxygen-containing polar groups such as epoxy, carboxyl and hydroxyl groups on the surface provides GO with excellent dispersity in polar solvents including water and creates the potential for further functionalization. By utilizing GO's huge surface area and its good dispersity in polar solvents, GO is a promising candidate for environmental applications and catalytic supports for novel metal nanoparticles.[22–24]

H. Yang, T. Kwon, Prof. B. J. Kim
Department of Chemical and Biomolecular Engineering
Korea Advanced Institute of Science and Technology (KAIST)
Daejeon, 305-701, Korea
E-mail: bumjoonkim@kaist.ac.kr
Y. Kwon, Prof. H. Lee
Department of Chemical and Biomolecular Engineering
Yonsei University
Seoul 120-749, Korea

DOI: 10.1002/smll.201201002

It is necessary to develop a technique for anchoring metal nanoparticles on GO to use GO as catalytic supports. Several experimental methods have been used to anchor metal nanoparticles on GO. The most popular approach involves the *in situ* reduction of a metal precursor on GO;[24–27] however, because of the inhomogeneous nature of metal reduction on GO, it is difficult to control the nanostructures of metal nanoparticles. One possible way to overcome some of these drawbacks is to use π–π stacking between a pre-formed nanoparticle and the GO. A particularly interesting example is the work of Huang and co-workers,[28] who showed π–π stacking between the GO and pyrene containing molecules bound to Au nanoparticles. However, unlike in covalent bonding, nanoparticles that are attached to GO by such a weak interaction can be easily detached from the GO during application. Additionally, this approach requires a particular type of surface-capping agent for the metal nanoparticles, which hinders the use of nanoparticles of various shapes and sizes. Another approach of 1-ethyl-3-(3-dimethylaminopropyl)carbodiimide (EDC) chemistry has been recently reported to graft the nanoparticles on GO.[29–31] The method requires amine functionalization on the nanoparticle surface to react with carboxylic groups on the GO. However, the approach has been limited to oxide type nanoparticles and the EDC reaction should be performed at low concentration of the reactants to prevent the aggregation of GO sheets.[31] Therefore, it is essential to develop an effective and universal approach to produce a metal nanoparticle-GO composite.

Click chemistry has been defined as a concept to achieve the universal linkage of chemical molecules.[32] Copper-catalyzed azide-alkyne cycloaddition (CuAAC) is an example of click chemistry. Due to its high reaction yield, high tolerance of functional groups, and mild reaction conditions, CuAAC has been used extensively for the functionalization of nanoparticles,[33–39] copolymer synthesis[40–42] and surface modification.[43,44] Although click chemistry has recently been used to immobilize polymers to graphene,[45,46] to our knowledge, the grafting of nanoparticles onto graphene or GO using click chemistry has not yet been reported.

This paper presents a simple and universal method of grafting nanoparticles onto the surface of a GO via a click reaction. For the model system, CuPt nanorods with a controlled size, aspect ratio (AR) and uniformity were carefully chosen and synthesized. The surface of the CuPt nanorods was then modified via a simple ligand exchange method using azide-functionalized ligands with a thiol end-group. Subsequently, it was coupled to the alkyne-functionalized GO (alkyne-GO) via a click reaction to produce a CuPt nanorod-grafted GO composite (CuPt-GO). To demonstrate the versatility of our approach, CuPt nanorods with ARs ranging from 1 to 11 were grafted onto the GO. CuPt nanorods were found to be distributed over the GO surface independent of the AR and size of the CuPt nanorods. This means that our approach can be applied to any shape or size of nanoparticle system generally. In addition, their catalytic properties in the water phase were investigated using a peroxidase-like o-phenylenediamine (OPD) oxidation reaction.

2. Results and Discussion

2.1. Preparation of Azide Functionalized CuPt Nanorods ($CuPt\text{-}N_3$) with Controlled ARs

CuPt nanorods with ARs of 1, 5, and 11 were produced with high monodispersity using a thermal decomposition process.[47,48] It is well known that the AR of inorganic nanorods can be controlled via the chosen capping agent.[49] In this study, an increase in the ratio of oleylamine (OLA) to oleic acid (OA) resulted in a higher nanorod AR. To obtain highly monodispersed nanorods with controlled ARs, as-synthesized nanorods were purified using a procedure from literatures.[47,48,50]

Figures 1a,b,c present transmission electron microscopy (TEM) images of CuPt nanorods with ARs of 1, 5 and 11, respectively. These images show that all of the OA- and OLA-coated CuPt nanorods were well-dispersed in hexane. It should be noted that as the long axis increased to 2.6, 14.0, and 27.7 nm for CuPt nanorods with ARs of 1, 5 and 11, respectively, the short axis for the nanorods remained constant at 2.6 nm. Therefore, this system is ideal for investigating the effect of AR on the properties of nanorods.

The azide functionalized CuPt ($CuPt\text{-}N_3$) nanorods were synthesized as follows. First, azide-functionalized ligands with a thiol end-group, 10-azidododecane-1-thiol, were synthesized from 11-bromo-1-undecene.[51] The azide-functionalized thiols were used to replace the surface-capping agents on the CuPt nanorod surface *via* a ligand exchange reaction because thiol-terminated ligands can bind to the surface of various inorganic nanoparticles (e.g., Au, Ag, Pt, etc.) more strongly than ligands with other functional end groups.[52–55] After the ligand exchange, all of the CuPt nanorods with different ARs were well dispersed in tetrahydrofuran (THF) without any aggregation or change in size or shape. For example, the TEM images in Figure 1a,d show the identical shapes and sizes of the CuPt nanorods (AR = 1) before and after azide functionalization. In addition, the attenuated total reflectance-Fourier transform infrared (ATR-FTIR) spectrum in **Figure 2** reveals the strong signal of $CuPt\text{-}N_3$ at 2100 cm^{-1}, which is a signature of the azide functional groups. Therefore, it can be concluded that the CuPt nanorods were successfully functionalized by azide-functionalized thiols.

2.2. Preparation and Characterization of a CuPt-GO Composite

The schematic procedure of our approach to produce CuPt-GO by click chemistry was illustrated in **Scheme 1**. First, the GO was prepared using the modified Hummers method.[56] The successful synthesis of GO can be confirmed using X-ray diffraction (XRD) and atomic force microscopy (AFM) measurements, as shown in the Supporting Information (SI), Figure S1. The XRD pattern of the synthesized GO exhibits a peak at $2\theta = 10.15°$, which corresponds to an interlayer d-spacing of 0.87 nm. This spacing is consistent with the values for GO reported in the literature.[57] The AFM image confirmed that the synthesized GO had a thickness of

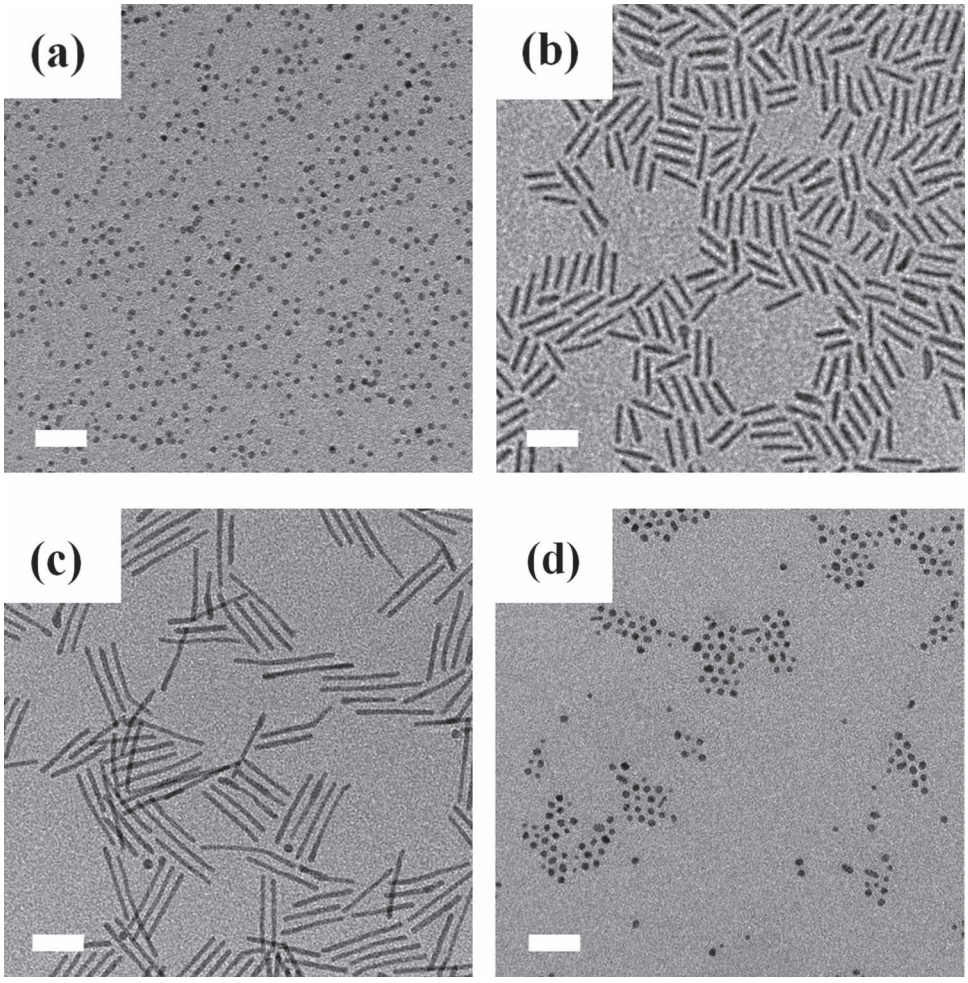

Figure 1. TEM images of OA/OLA-coated CuPt nanorods with ARs of (a) 1, (b) 5 and (c) 11. (d) CuPt-N_3 nanorods (AR = 1) dispersed in THF. Scale bar is 20 nm.

approximately 0.8 nm. Then, a two-step approach was used to graft the alkyne groups to the GO via an acylation reaction of carboxylic acid on the GO surface. Finally, during the click reaction step, CuPt-N_3 nanorods were added and reacted in high yield with the alkyne groups on the GO surface. Subsequently, unreacted CuPt nanorods were thoroughly removed via repeated washing with THF and dimethylformamide (DMF).

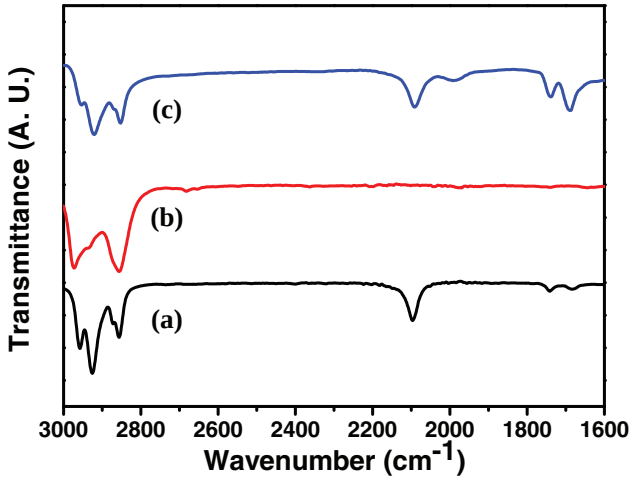

Figure 2. ATR-FTIR spectra of (a) 10-azidodecane-1-thiol, (b) OA/OLA-coated CuPt nanorods (AR = 5) and (c) CuPt-N_3 nanorods (AR = 5). In (c), the peak at ~2100 cm^{-1} shows the presence of the azide groups on the CuPt-N_3 surface.

Figure 3 shows TEM images of CuPt-GO. To demonstrate the effectiveness of our universal approach, CuPt nanorods with different ARs were attached to the GO using click chemistry. Independent of shape or size, the CuPt-N_3 nanorods could be attached to the alkyne-GO surface by formation of covalent linkages. CuPt nanorods were also found to be distributed over the entire GO surface, including the edges and basal planes of the GO. In a control experiment, the alkyne-GO was reacted under the same conditions as the CuPt-GO preparation using unmodified OA/OLA coated CuPt nanorods. After the reaction, however, no grafted CuPt nanorods were found on the GO surface. The results demonstrate the importance of our click reaction in producing CuPt-GO composites.

To monitor the progress in the formation of alkyne-GO and its click reaction with CuPt-N_3, ATR-FTIR spectra of (a) GO, (b) alkyne-GO, (c) CuPt-N_3 and (d) CuPt-GO were taken and compared. (**Figure 4** and SI, Figure S2) A comparison of

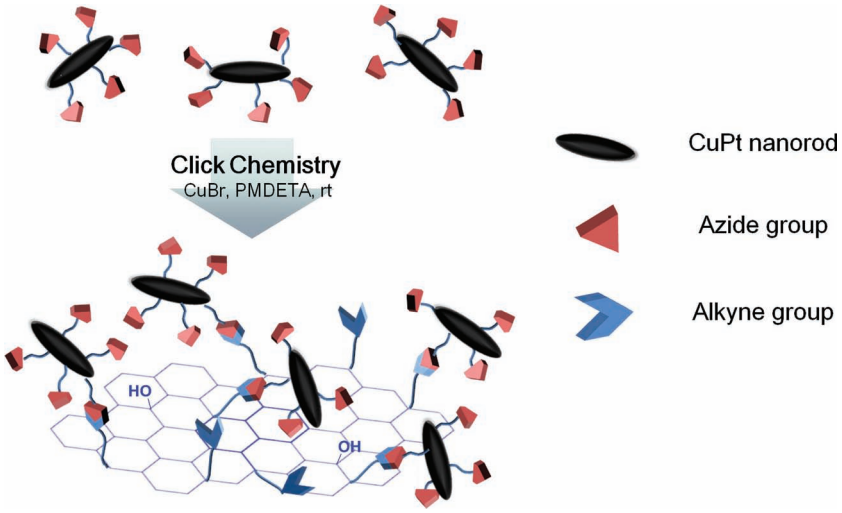

Scheme 1. Schematic illustration of our "click" approach to producing CuPt-GO.

the FTIR spectra in SI, Figure S2a,b shows that new peaks occur between 2800 and 3000 cm^{-1} after the alkyne modification of the GO. These peaks occur due to alkyl stretching vibrations from the alkyl group between the alkyne and ester groups (SI, Figure S2), indicating the successful grafting of the alkyne group onto the GO. The ATR-FTIR spectra of the CuPt-N_3 nanorods in Figure 4c show a strong peak at 2100 cm^{-1}, which is a signature of the azide functional groups on the nanorod surface. After the click reaction between the alkyne-GO and CuPt-N_3, as shown in Figure 4d, the peak at 2100 cm^{-1} is almost disappeared. Instead, a strong signal with a peak at 1640 cm^{-1} was found, which is a signature of triazole ring that is formed by click reaction between the CuPt-N_3 nanorods and the alkyne-GO.[58]

The X-ray photoelectron spectroscopy (XPS) spectra prove the formation of the CuPt-GO and monitor the completion of each reaction step. **Figure 5**b shows a peak at 399 eV in the N1s spectrum of the OA/OLA-coated CuPt nanorods due to NH_2 functional groups of OLA on the CuPt nanorods.[59] The XPS spectrum of the CuPt-N_3 nanorods in Figure 5c shows two peaks at 404.5 eV and 400 eV, which confirms the presence of azide groups on the nanorods.[44] In particular, the intensity ratio of the peak at 400 eV to that at 399 eV is very large, indicating that the ligand exchange procedures by the azide groups on the CuPt nanorods were highly effective. The intensity ratios of the peaks at 404.5 eV and 400 eV in Figure 5c,d were compared to monitor the progress of the click reaction between the CuPt-N_3 and the alkyne GO. Whereas the intensity ratio was 1:2 (404.5 eV to 400 eV) in the CuPt-N_3 nanorods, the peak intensity at 404.5 eV decreased significantly after the click reaction, causing the peak intensity ratio to decrease to 1:5. (Figure 5d) Because the triazole ring (a click product derived from the azide and alkyne groups) shows a signal only at 400 eV,[60] the peak intensity at 404.5 eV decreases significantly as the azide group is transformed into the trizole ring. This proves that click reaction has been successful, which is consistent with the previous ATR-FTIR results.

It is worth noting that our click chemistry-based system has unique advantages. First, azide-functionalized thiols can be easily attached to any shape and any species of metal nanoparticle through a simple ligand exchange. Usually, method of *in situ* growth of nanoparticle on the GO surface can make only one species of nanoparticle such as Au and Pt.[24,61] However, with our method, it is possible to attach bimetallic nanoparticles (i.e., CuPt). This means that we can introduce a variety of functional properties to the nanoparticle-GO composite. In addition, our approach provides much better control in the characteristics and dispersion of nanoparticles on the GO compared to the *in situ* growth of nanoparticles on the GO surface.[24] Furthermore, unlike other reactions, our click approach can function under very mild reaction conditions (e.g., at room temperature), thus preventing any aggregation or degradation of nanoparticles during the reaction.

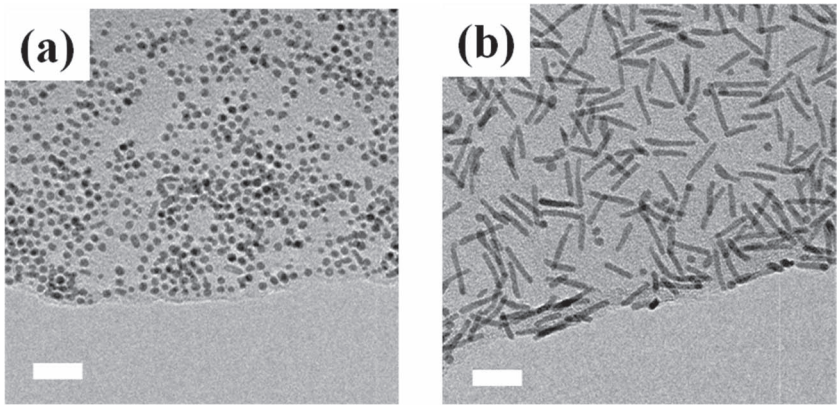

Figure 3. TEM images of CuPt-GO with anchored CuPt nanorods of different ARs. (a) CuPt-GO (AR = 1) and (b) CuPt-GO (AR = 5). Scale bar is 20 nm.

2.3. Catalytic Behavior of CuPt-GO Composites

As shown in the previous report, Pt alloy nanoparticles are known to catalyze the decomposition of superoxide free radicals and H_2O_2.[62] The shape, size and composition of Pt alloy nanoparticles are critical in determining their catalytic properties, and nanoparticles with the appropriate properties are typically synthesized using organic materials such as stabilizing ligands, which makes the nanoparticles only soluble in organic solvents.[63,64] However, the use of polar solvents (and water in particular) for nanoparticle applications is important due to environmental, economical and safety concerns.

NANO MICRO small

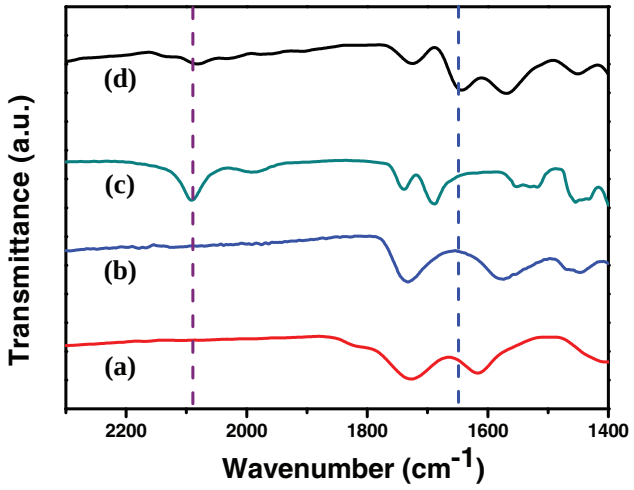

Figure 4. ATR-FTIR spectra of (a) GO, (b) alkyne-GO, (c) CuPt-N_3 nanorods and (d) CuPt-GO.

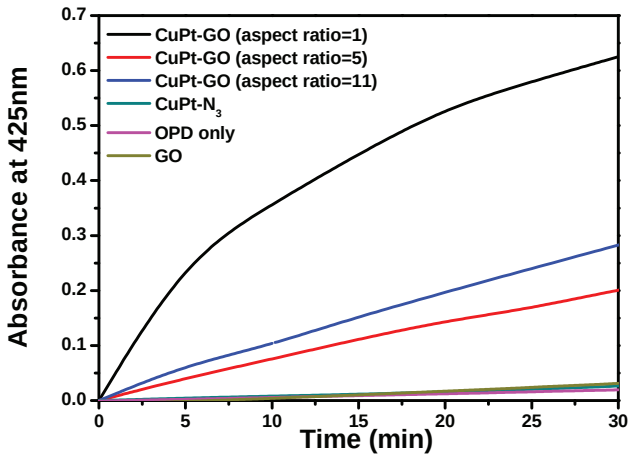

Figure 6. OPD oxidation using CuPt-GO with various CuPt ARs as catalysts was monitored by UV-Vis absorbance measurements at 425 nm as a function of reaction time. CuPt-N_3 and unfunctionalized GO were used as the control.

In the present case, a peroxidase-like OPD oxidation reaction was obtained with a CuPt-GO composite as a catalyst in the aqueous phase because GO is able to function in polar solvents as a catalytic support for CuPt nanorods. This type of enzyme-mimicking reaction occurs in the aqueous phase, where OPD is oxidized into a yellow solution of 2,3-diaminophenazine during the reaction. UV-Vis spectroscopy is used to monitor the progress of the OPD reaction by measuring the increase in peak intensity at 425 nm. To confirm that CuPt nanorods with various ARs show catalytic activity even when immobilized on GO, the OPD oxidation reaction was performed using the same Pt amount in each sample. The UV-Vis absorbance spectrum in **Figure 6** demonstrates that GO without CuPt nanorods shows no catalytic activity. The UV-Vis absorbance spectra of the unmodified GO were similar to those of OPD reactions without catalysts. In contrast, CuPt-GO with various CuPt ARs exhibited a drastic increase in absorbance at 425 nm. This means that the CuPt nanorods on the GO acted as catalysts in the oxidation of OPD in the aqueous phase, and the GO was successfully used as a catalytic nanorod support for organic transformations. CuPt nanoparticle-GO (AR = 1) showed higher catalytic property than other CuPt nanorod-GO (ARs = 5 and 11). These results are consistent with our previous research, which showed that CuPt nanoparticles (AR = 1) exhibited greater catalytic activity than did CuPt nanorods (ARs = 5 and 11) because of the difference in Pt composition on the surface of the nanorods.[48] For control experiment, the catalytic properties of ungrafted CuPt-N_3 nanoparticles (AR = 1) in water were measured to compare the effect of immobilization via 'click chemistry'. The catalytic reaction was performed under identical condition to that for CuPt-GO. The amount of CuPt-N_3 nanoparticles (AR = 1) was controlled to contain 170 μM of Pt in 2.85 ml water, which is exactly same amount and concentration of Pt used in the catalytic experiment of CuPt-GO. As shown in Figure 6, the UV-Vis absorbance spectra of CuPt-N_3 nanoparticles (AR = 1) are same as those of OPD reactions without any reagent, indicating that CuPt-N_3 nanoparticles (AR = 1) do not show any catalytic activities. This result is due to severe aggregation of the unattached nanoparticles in water phase. This demonstrates that CuPt nanoparticles attached on GO are solely responsible for catalytic properties for CuPt-GO samples.

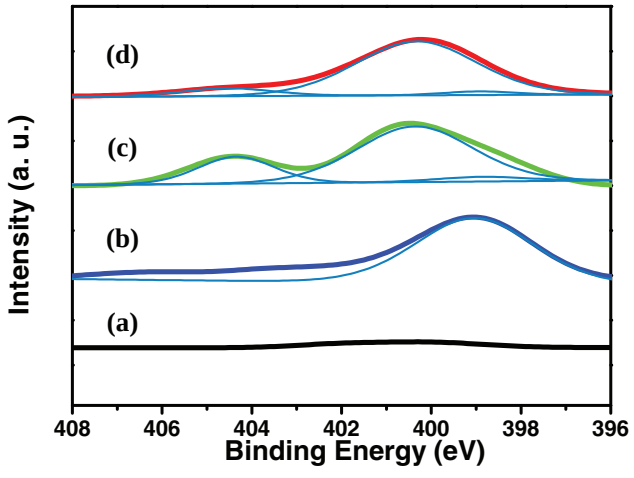

Figure 5. N1s XPS spectra of (a) alkyne-GO, (b) OA/OLA coated CuPt, (c) CuPt-N_3 nanorods (AR = 5) and (d) CuPt-GO (AR = 5).

3. Conclusion

In this study, an effective approach to preparing CuPt-GO was developed using click chemistry. CuPt nanorods with various ARs were synthesized by thermal decomposition. Using simple ligand exchange, CuPt nanorods were functionalized with azide groups. The CuPt nanorods were then anchored to the GO without aggregation. This approach affords a facile means of anchoring various shapes and sizes of nanorods on the GO. Although CuPt nanorods are originally nonpolar, because of oxygen-containing groups on the GO, CuPt-GO was successfully employed in catalytic reaction of OPD oxidation in water phase. This result demonstrates that

nonpolar CuPt nanorods on GOs exhibit catalytic activity in the aqueous phase and that GO can be used as a catalytic nanorod support for organic transformation. Considering the potential applications of nanoparticle-GO composites, we believe that this approach can be easily extended to design other functional nanoparticles with graphene for electronic and environmental applications.

4. Experimental Section

Materials: 11-bromo-1-undecene, thioacetic acid, sodium azide, acetyl chloride, copper acetylacetonate ($Cu(acac)_2$), platinum acetylacetonate ($Pt(acac)_2$), 1,2-hexadecanediol, OA, OLA, 1-octadecene, OPD, potassium persulfate, phosphorus pentoxide, triethylamine (TEA), propargyl alcohol, copper bromide (CuBr), and *N,N,N′,N″,N‴*-Pentamethyldiethylenetriamine (PMDETA) were purchased from Sigma-Aldrich. Azobisisobutyronitrile (AIBN) and $KMnO_4$ are purchased from Junsei. Graphite powders are purchased from Graphit Kropfmuhl.

Synthesis of 11-(Bromoundecyl)thioacetate: 11-bromo-1-undecene (2.0 g, 8.58 mmol), thioacetic acid (3.3 g, 42.9 mmol), and AIBN (704 mg, 4.29 mmol) were dissolved in toluene (50 mL). A flow of argon was bubbled through the reaction for 1 hr. Then, the mixture was stirred at the reflux temperature for 4 hrs under argon atmosphere. The resulting mixture was diluted with diethyl ether (200 mL) and the separated organic layer was washed with DI water and brine, dried over $MgSO_4$, and concentrated *in vacuo*. The crude product was purified by column chromatography on silica gel using hexane: CH_2Cl_2 (2:1) as the eluent to yield 11-(bromoundecyl)thioacetate (2.31 g, 87%) as a colorless oil. ^{1}H NMR (300 MHz, $CDCl_3$,δ): 3.41 (t, 2H, J = 6.9 Hz, CH_2-Br), 2.86 (t, 2H, J = 7.2 Hz, CH_2-S), 2.32 (s, 3H, CO-CH_3), 1.85 (q of t, 2H, J = 7.8 Hz, Br-CH_2-CH_2), 1.56 (m, 2H, S-CH_2-CH_2), 1.27 (m, 14H).

Synthesis of 11-(Azidoundecyl)thioacetate: 11-(bromoundecyl) thioacetate (450 mg, 1.45mmol), sodium azide (805.5 mg, 12.3mmol) were dissolved in DMF (10 mL). The mixture was heated to 60 °C for 10 hrs. The DMF was removed under vacuum and the resulting crude was dissolved in CH_2Cl_2 and washed with DI water and brine. The organic layer was dried over $MgSO_4$ and the solvent was removed *in vacuo* to yield 11-(azidoundecyl)thioacetate (378 mg, 96%). ^{1}H NMR (300 MHz, $CDCl_3$,δ): 3.19 (t, 2H, J = 8.8 Hz, CH_2-N_3), 2.79 (t, 2H, J = 7.2 Hz, CH_2-S), 2.25 (s, 3H, CO-CH_3), 1.51 (m, 2H, CH_2-CH_2-S), 1.20 (m, 16H).

Synthesis of 10-Azidodecane-1-thiol: 11-(azidoundecyl)thioacetate (378 mg, 1.39 mmol) was dissolved in anhydrous methanol (10 mL). Acetyl chloride (1 mL) was then added dropwise to the solution under argon atmosphere and at 0 °C. The subsequent solution was allowed to warm to room temperature for 3 hrs, and the resulting mixture was diluted with diethyl ether. The separated organic layer was washed with DI water and brine, dried over $MgSO_4$. The combined organic layer was concentrated under vacuum to give product (276.7 mg, 86.8%). ^{1}H NMR (300 MHz, $CDCl_3$,δ): 3.19 (t, 2H, J = 6.8 Hz, CH_2-N_3), 2.46 (q, 2H, J = 7.3 Hz, CH_2-S), 1.54 (m, 6H), 1.21 (m, 16H).

Synthesis of CuPt Nanorods with Various ARs: CuPt nanorods were synthesized by the thermal degradation method with the standard air free technique.[47,48] Typically, $Cu(acac)_2$ (24 mg) and $Pt(acac)_2$ (43 mg) were dissolved in 1-octadecene (5 mL). OA and OLA as capping agents (OA (1.5 mL) for spherical nanoparticles, OLA (0.8 mL) and OA (0.6 mL) for short nanorods, OLA (1.2 mL) and OA (0.8 mL) for long nanorods) and 1,2-hexadecanediol as the reducing agent (105 mg) were added to the reaction mixture. The solution was heated and stirred at 120 °C under a nitrogen atmosphere for 20 min to melt the precursors. The temperature was then increased to 225 °C and maintained for 30 min to prepare the product. The solution was cooled down to room temperature, and the product was precipitated in ethanol by centrifugation at 3600 rpm for 10 min. This sequence of steps afforded a precipitate that could be dispersed in hexane, cyclohexane and toluene. To purify synthesized nanorods, two different purification steps were performed. In the first step, synthesized nanorods were dispersed in a 50: 50 mixture of hexane and acetone and the desired product was separated by precipitation at 3600 rpm. In the second step, the density-gradient method was used for complete purification by following previous literatures.[47,48,50]

Ligand Exchange to Form CuPt-N_3 Nanorods: The CuPt nanorods and 10-azidodecane-1-thiol molecules (37 mg and 26 mg for spherical nanoparticles, 27 mg and 12.4 mg for short nanorods, 40 mg and 21.5 mg for long rods, respectively) were mixed in toluene (10 mL) at 40 °C for 2 days under argon atmosphere. Then, CuPt nanorods were washed several times with hexane to remove residual unattached ligands.

Preparation of Alkyne-GO: The GO was synthesized using a modified Hummers method.[56] The alkyne-GO was prepared following a procedure from the literature.[45] The GO (100 mg) was refluxed in $SOCl_2$ (20 mL) at 70 °C for 24 h. After the excess $SOCl_2$ had been removed under reduced pressure, the products were dried *in vacuo*. Propargyl alcohol (2 mL), distilled dichloromethane (2 mL) and triethylamine (1 mL) were added dropwise at 0 °C. The mixture was stirred at 0 °C for 1 h and then at room temperature for 24 h. The powders were washed with an excess amount of ethanol and DI water. After washing, the resulting powders were dried *in vacuo* overnight.

Click Reaction of CuPt-N_3 with Alkyne-GO via a CuAAC Reaction: Terminal alkyne-GO (20 mg), CuPt-N_3 nanorods (20 mg), CuBr (6.2 mg, 0.043 mmol), PMDETA (10 μL, 0.051 mmol), DMF (distilled, 15 mL), and THF (5 mL) were added to a 50 mL flask. After degassing, the reaction mixture was stirred under nitrogen at room temperature for 48 hrs. As the CuAAC reaction finished, the mixture was dissolved in THF and DMF and filtered through a 220 nm PTFE membrane for several times. The collected powders were dried *in vacuo*.

Oxidation Reaction of OPD: The catalytic property of the CuPt-GO was measured using a modified procedure from the literature.[48] CuPt-GO composites with CuPt nanorods with various ARs were used as catalysts in the oxidation of OPD in the presence of H_2O_2. An oxidation reaction was preceded in the H_2O solution. Each type of CuPt-GO was dispersed in H_2O (2.85 mL). Then, 30% H_2O_2 (100 μL) and 0.02 M OPD (50 μL) were added to the H_2O solution, and the total volume of the solution was maintained at 3 mL. The amount of Pt in the solution was kept constant at 170 μM. Based on the inductively coupled plasma (ICP) analysis of Pt in the CuPt-GO, the amount of each type of CuPt-GO was controlled to determine the effect of the AR on the catalytic property. The progress of the oxidation reaction was monitored at room temperature by recording UV-Vis absorption spectra at 5 min intervals using the scanning kinetics mode.

NANO MICRO small

Characterization: TEM studies were performed to investigate the size and shape of the CuPt nanorods and to observe the morphology of the CuPt-GO using a JEOL 2000FX. ATR-FTIR spectra were taken using a Bruker ALPHA. XPS spectra were taken using a Thermo VG Scientific ESCA 2000. XRD measurements were performed using a RIGAKU D/MAX-IIIC (3kW) with Cu-Kα radiation (λ = 0.154 nm). The GO was examined via AFM using a PSIA XE-100 in a non-contacting mode. For imaging, the GO was dissolved in water and then spin-coated onto an Si-wafer. ICP was used to measure the quantity of Pt in the CuPt-GO using a Thermo IRIS Intrepid II XSP. UV-Vis absorption spectra were taken using a SCINCO S-3100 spectrometer equipped with quartz cells.

Supporting Information

Supporting Information is available from the Wiley Online Library or from the author.

Acknowledgements

This research was supported by the Korea Research Foundation Grant, funded by the Korean Government (2011-0027240). We thank Prof. Doh Chang Lee and his student, Chaewon Pak for the help in the XRD measurement.

[1] W. U. Huynh, J. J. Dittmer, A. P. Alivisatos, *Science* **2002**, *295*, 2425.
[2] D. L. Feldheim, K. C. Grabar, M. J. Natan, T. E. Mallouk, *J. Am. Chem. Soc.* **1996**, *118*, 7640.
[3] S. H. Sun, C. B. Murray, D. Weller, L. Folks, A. Moser, *Science* **2000**, *287*, 1989.
[4] H. B. Na, J. H. Lee, K. J. An, Y. I. Park, M. Park, I. S. Lee, D. H. Nam, S. T. Kim, S. H. Kim, S. W. Kim, K. H. Lim, K. S. Kim, S. O. Kim, T. Hyeon, *Angew. Chem. Int. Ed.* **2007**, *46*, 5397.
[5] C. Besson, E. E. Finney, R. G. Finke, *J. Am. Chem. Soc.* **2005**, *127*, 8179.
[6] S. Eustis, M. A. El-Sayed, *Chem. Soc. Rev.* **2006**, *35*, 209.
[7] A. R. Tao, S. Habas, P. D. Yang, *Small* **2008**, *4*, 310.
[8] R. Hong, N. O. Fischer, T. Emrick, V. M. Rotello, *Chem. Mater.* **2005**, *17*, 4617.
[9] T. Kwon, T. Kim, F. B. Ali, D. J. Kang, M. Yoo, J. Bang, W. Lee, B. J. Kim, *Macromolecules* **2011**, *44*, 9852.
[10] J. A. Lopez-Sanchez, N. Dimitratos, C. Hammond, G. L. Brett, L. Kesavan, S. White, P. Miedziak, R. Tiruvalam, R. L. Jenkins, A. F. Carley, D. Knight, C. J. Kiely, G. J. Hutchings, *Nat. Chem.* **2011**, *3*, 551.
[11] A. Dong, X. Ye, J. Chen, Y. Kang, T. Gordon, J. M. Kikkawa, C. B. Murray, *J. Am. Chem. Soc.* **2010**, *133*, 998.
[12] R. Tangirala, J. L. Baker, A. P. Alivisatos, D. J. Milliron, *Angew. Chem. Int. Ed.* **2010**, *49*, 2878.
[13] D. J. Kang, T. Kwon, M. P. Kim, C. H. Cho, H. Jung, J. Bang, B. J. Kim, *ACS Nano* **2011**, *5*, 9017.
[14] M. V. Kovalenko, M. Scheele, D. V. Talapin, *Science* **2009**, *324*, 1417.
[15] K. Paek, S. Chung, C. H. Cho, B. J. Kim, *Chem. Commun.* **2011**, *47*, 10272.
[16] M. Terrones, O. Martín, M. González, J. Pozuelo, B. Serrano, J. C. Cabanelas, S. M. Vega-Díaz, J. Baselga, *Adv. Mater.* **2011**, *23*, 5302.
[17] X. Y. Yang, X. Y. Zhang, Y. F. Ma, Y. Huang, Y. S. Wang, Y. S. Chen, *J. Mater. Chem.* **2009**, *19*, 2710.
[18] Y. J. Gan, L. T. Sun, F. Banhart, *Small* **2008**, *4*, 587.
[19] G. Eda, G. Fanchini, M. Chhowalla, *Nat. Nanotechnol.* **2008**, *3*, 270.
[20] K. S. Kim, Y. Zhao, H. Jang, S. Y. Lee, J. M. Kim, K. S. Kim, J. H. Ahn, P. Kim, J. Y. Choi, B. H. Hong, *Nature* **2009**, *457*, 706.
[21] D. Li, M. B. Muller, S. Gilje, R. B. Kaner, G. G. Wallace, *Nat. Nanotechnol.* **2008**, *3*, 101.
[22] S. T. Yang, Y. L. Chang, H. F. Wang, G. B. Liu, S. Chen, Y. W. Wang, Y. F. Liu, A. N. Cao, *J. Colloid. Interf. Sci.* **2010**, *351*, 122.
[23] I. V. Lightcap, T. H. Kosel, P. V. Kamat, *Nano Lett* **2010**, *10*, 577.
[24] N. Zhang, H. X. Qiu, Y. Liu, W. Wang, Y. Li, X. D. Wang, J. P. Gao, *J. Mater. Chem.* **2011**, *21*, 11080.
[25] C. Xu, X. Wang, J. W. Zhu, *J. Phys. Chem. C* **2008**, *112*, 19841.
[26] G. Goncalves, P. A. A. P. Marques, C. M. Granadeiro, H. I. S. Nogueira, M. K. Singh, J. Gracio, *Chem. Mater.* **2009**, *21*, 4796.
[27] X. Z. Zhou, X. Huang, X. Y. Qi, S. X. Wu, C. Xue, F. Y. C. Boey, Q. Y. Yan, P. Chen, H. Zhang, *J. Phys. Chem. C* **2009**, *113*, 10842.
[28] J. Huang, L. Zhang, B. Chen, N. Ji, F. Chen, Y. Zhang, Z. Zhang, *Nanoscale* **2010**, *2*, 2733.
[29] F. A. He, J. T. Fan, D. Ma, L. M. Zhang, C. Leung, H. L. Chan, *Carbon* **2010**, *48*, 3139.
[30] Y. Zhang, B. A. Chen, L. M. Zhang, J. Huang, F. H. Chen, Z. P. Yang, J. L. Yao, Z. J. Zhang, *Nanoscale* **2011**, *3*, 1446.
[31] Q. Liu, J. B. Shi, J. T. Sun, T. Wang, L. X. Zeng, G. B. Jiang, *Angew. Chem. Int. Ed.* **2011**, *50*, 5913.
[32] M. Gragert, M. Schunack, W. H. Binder, *Macromol. Rapid. Commun.* **2011**, *32*, 419.
[33] E. Drockenmuller, I. Colinet, D. Damiron, F. Gal, H. Perez, G. Carrot, *Macromolecules* **2010**, *43*, 9371.
[34] J. L. Brennan, N. S. Hatzakis, T. R. Tshikhudo, N. Dirvianskyte, V. Razumas, S. Patkar, J. Vind, A. Svendsen, R. J. M. Nolte, A. E. Rowan, M. Brust, *Bioconj. Chem.* **2006**, *17*, 1373.
[35] R. Ranjan, W. J. Brittain, *Macromolecules* **2007**, *40*, 6217.
[36] D. A. Fleming, C. J. Thode, M. E. Williams, *Chem. Mater.* **2006**, *18*, 2327.
[37] T. Zhang, Z. H. Zheng, X. B. Ding, Y. X. Peng, *Macromol. Rapid. Commun.* **2008**, *29*, 1716.
[38] J. Lim, H. Yang, K. Paek, C. H. Cho, S. Kim, J. Bang, B. J. Kim, *J. Polym. Sci. Pol. Chem.* **2011**, *49*, 3464.
[39] E. Boisselier, L. Salmon, J. Ruiz, D. Astruc, *Chem. Commun.* **2008**, 5788.
[40] A. J. D. Magenau, N. Martinez-Castro, D. A. Savin, R. F. Storey, *Macromolecules* **2009**, *42*, 8044.
[41] E. D. Pressly, R. J. Amir, C. J. Hawker, *J. Polym. Sci. Pol. Chem.* **2011**, *49*, 814.
[42] W. C. Lin, Q. Fu, Y. Zhang, J. L. Huang, *Macromolecules* **2008**, *41*, 4127.
[43] X. Ru, X. H. Zeng, Z. M. Li, D. J. Evans, C. X. Zhan, Y. Tang, L. J. Wang, X. M. Liu, *J. Polym. Sci. Pol. Chem.* **2010**, *48*, 2410.
[44] J. P. Collman, N. K. Devaraj, T. P. A. Eberspacher, C. E. D. Chidsey, *Langmuir* **2006**, *22*, 2457.
[45] S. Sun, Y. Cao, J. Feng, P. Wu, *J. Mater. Chem.* **2010**, *20*, 5605.
[46] Y. Z. Pan, H. Q. Bao, N. G. Sahoo, T. F. Wu, L. Li, *Adv. Funct. Mater.* **2011**, *21*, 2754.
[47] Q. S. Liu, Z. Yan, N. L. Henderson, J. C. Bauer, D. W. Goodman, J. D. Batteas, R. E. Schaak, *J. Am. Chem. Soc.* **2009**, *131*, 5720.
[48] T. Kwon, M. Min, H. Lee, B. J. Kim, *J. Mater. Chem.* **2011**, *21*, 11956.
[49] Y. H. Wei, S. Chen, B. Kowalczyk, S. Huda, T. P. Gray, B. A. Grzybowski, *J. Phys. Chem. C* **2010**, *114*, 15612.
[50] L. Bai, X. Ma, J. Liu, X. Sun, D. Zhao, D. G. Evans, *J. Am. Chem. Soc.* **2010**, *132*, 2333.
[51] W. J. Sommer, M. Weck, *Langmuir* **2007**, *23*, 11991.
[52] S. F. Wuister, I. Swart, F. van Driel, S. G. Hickey, C. D. Donega, *Nano Lett.* **2003**, *3*, 503.

[53] X. C. Sun, C. J. Thode, J. K. Mabry, J. W. Harrell, D. E. Nikles, K. Sun, L. M. Wang, *J. Appl. Phys.* **2005**, *97*, 10Q901.
[54] N. R. Jana, X. G. Peng, *J. Am. Chem. Soc.* **2003**, *125*, 14280.
[55] J. B. He, P. Kanjanaboos, N. L. Frazer, A. Weis, X. M. Lin, H. M. Jaeger, *Small* **2010**, *6*, 1449.
[56] W. S. Hummers, R. E. Offeman, *J. Am. Chem. Soc.* **1958**, *80*, 1339.
[57] A. J. Patil, J. L. Vickery, T. B. Scott, S. Mann, *Adv. Mater.* **2009**, *21*, 3159.
[58] S. K. Yadav, S. S. Mahapatra, J. W. Cho, J. Y. Lee, *J. Phys. Chem. C* **2010**, *114*, 11395.
[59] B. Koo, J. Park, Y. Kim, S. H. Choi, Y. E. Sung, T. Hyeon, *J. Phys. Chem. B* **2006**, *110*, 24318.
[60] A. Devadoss, C. E. D. Chidsey, *J. Am. Chem. Soc.* **2007**, *129*, 5370.
[61] Y. J. Li, W. Gao, L. J. Ci, C. M. Wang, P. M. Ajayan, *Carbon* **2010**, *48*, 1124.
[62] W. W. He, X. C. Wu, J. B. Liu, X. N. Hu, K. Zhang, S. A. Hou, W. Y. Zhou, S. S. Xie, *Chem. Mater.* **2010**, *22*, 2988.
[63] X. Teng, X. Liang, S. Maksimuk, H. Yang, *Small* **2006**, *2*, 249.
[64] C. Wang, H. Daimon, Y. Lee, J. Kim, S. Sun, *J. Am. Chem. Soc.* **2007**, *129*, 6974.

Received: May 8, 2012
Published online: July 23, 2012

